Remote Sensing of Environment 209 (2018) 456–467

Contents lists available at ScienceDirect

Remote Sensing of Environment

journal homepage: www.elsevier.com/locate/rse

Linking canopy scattering of far-red sun-induced chlorophyll fluorescence with reflectance

Peiqi Yang*, Christiaan van der Tol

Faculty of Geo-Information Science and Earth Observation (ITC), University of Twente, PO Box 217, AE Enschede 7500, The Netherlands

ARTICLE INFO

Keywords:
Sun-induced chlorophyll fluorescence
Canopy scattering
Reflectance
Leaf albedo
SCOPE
Canopy interceptance

ABSTRACT

Remotely sensed sun-induced chlorophyll fluorescence (SIF) has been used as an indicator of global terrestrial vegetation photosynthesis. The connection between SIF and photosynthesis allows its use for improving estimates of gross primary production (GPP) and monitoring plant stress. In these analyses, up-scaling of the relationship between SIF and photosynthesis from the photosynthetic level to the canopy, regional or global scale has been one of the main challenges. The scaling is strongly affected by the radiative transfer of emitted SIF, notably scattering and re-absorption of SIF. It is essential to understand these processes in order to differentiate effects of canopy structural variation from effects of photosynthesis functional variation on SIF. In this study, we derive the relationship between canopy scattering of SIF and top-of-canopy (TOC) reflectance analytically, by investigating the radiative transfer of incident light and emitted SIF. The similarity of radiative transfer of intercepted incident light and emitted SIF results in a simple relationship between reflectance and canopy scattering of SIF. In particular, we find that the ratio of far-red reflectance (R) to the product of canopy interceptance (i_0) and leaf albedo (ω) is an accurate estimate of canopy scattering of far-red SIF (i.e.,). SCOPE model simulations are used to validate our findings. The relationship we found provides an easy and accurate approach for rapid decoupling canopy structural and functional regulation of SIF, and correction of SIF for bidirectional effects. This will improve estimates of canopy photosynthesis from SIF.

1. Introduction

Sun-induced chlorophyll fluorescence (SIF) is a novel remote sensing signal for monitoring vegetation photosynthesis. It takes place in the pigment beds of photosystems, and SIF is an indicator of the efficiency by which photons are transmitted to photochemical reaction centers (Grace et al., 2007; Meroni et al., 2009). It is therefore closely related to the light harvesting process and responds timely to rapid changes in photosynthesis (Krause and Weis, 1991; Baker, 2008). In recent studies SIF was used to estimate vegetation photosynthetic capacity (Zhang et al., 2014) and for tracking dynamic changes of photosynthesis (Rossini et al., 2015). The connection between SIF and photosynthesis allows its use for improving the estimation of global or regional gross primary production (GPP) (Frankenberg et al., 2011; Guanter et al., 2014), and as an early warning signal of vegetation stress (Ač et al., 2015).

Apart from photosynthetic activity, SIF observations from remote sensing are strongly affected by the structure of vegetation canopies (Grace et al., 2007; Migliavacca et al., 2017; Damm et al., 2015). SIF observed at top of canopy is only a portion of the total emitted SIF, due to re-absorption and scattering (i.e., they are complementary to each other) (Porcar Castell et al., 2014). The scattering and re-absorption of SIF from the moment of emission to the moment of escape from the canopy in observation direction, is (among other factors) sensitive to canopy leaf area index (LAI) and leaf orientation (Verrelst et al., 2015; Verrelst et al., 2016). Scattering and re-absorption effects are spectrally dependent. SIF at 760 nm (far-red SIF) is scattered more and re-absorbed less than SIF at 687 nm (red SIF) (Porcar Castell et al., 2014) and therefore the portion of SIF reaching the sensor is higher for far-red SIF than for red SIF. As a result, the ratio of red and far-red SIF from canopy observation differs from that of leaf-level measurements (Fournier et al., 2012; Cendrero-Mateo et al., 2015).

Understanding of canopy scattering of SIF is crucial, especially when a quantitative link between SIF and photosynthesis is desired for GPP estimates. In a regional SIF to GPP comparison, Guanter et al. (2014) assumed a canopy scattering coefficient of unity (i.e. no absorption) of far-red SIF due to lack of effective ways to quantify the scattering, but acknowledged the potential importance of accurate estimates of this process. Simulations with radiative transfer models (RTMs) confirmed that the scattering is an important aspect: They show

* Corresponding author.
E-mail address: p.yang@utwente.nl (P. Yang).

https://doi.org/10.1016/j.rse.2018.02.029
Received 11 October 2017; Received in revised form 14 February 2018; Accepted 20 February 2018
Available online 19 March 2018
0034-4257/

that the relation between photosynthetic activity and SIF is canopy structure dependent (Damm et al., 2015; Verrelst et al., 2016) and that a substantial portion of the variability of SIF at different spatial and temporal scales is due to canopy structure rather than photosynthetic functioning (Koffi et al., 2015; Van der Tol et al., 2016; Migliavacca et al., 2017).

One way to study the effect of the scattering is to compare leaf-level and canopy-level measurements. Cendrero-Mateo et al. (2015) found that top-of-canopy (TOC) fluorescence of a wheat canopy measured in a growing season differed from leaf-average fluorescence, and that they developed differently over the growing season. The asymmetric evolution of leaf and canopy SIF may be attributed to seasonal changes in the scattering of fluorescence. Spectral differences between leaf and canopy SIF have also been reported. Fournier et al. (2012) reported that the ratio of red to far-red SIF of grass decreased by a factor of two from the leaf to the canopy level. This confirms that canopy scattering for the red and far-red SIF are different.

The empirical method (i.e. comparing leaf and canopy measurements) can reveal the magnitude of the effect of scattering in specific cases, but it is challenging to generalize the results. The need to sample a representative number of leaves that account for the variability of incident light and leaf properties makes the method labor intensive (Zarco-Tejada et al., 2003; Cendrero-Mateo et al., 2015). Furthermore, it is not easy to control the experiment and to identify and isolate the different effects on scattering, such as those of soil background, viewing and solar illumination angles.

RTMs offer a comprehensive complementary method to investigate the effects of canopy structure on TOC SIF. They provide an estimation of canopy scattering of SIF by simulating the light-canopy interaction. The SCOPE model (Van der Tol et al., 2009) simulates leaf fluorescence emission and TOC SIF, reflectance and photosynthesis of homogeneous canopies, while the mSCOPE model (Yang et al., 2017) simulates these for vertically heterogeneous canopies. For more complex canopies, 3D models have been developed, such as the DART (Gastellu-Etchegorry et al., 2017), FluorWPS (Zhao et al., 2016), and FluorFLIGHT (Hernández-Clemente et al., 2017). All these models require prior inputs of canopy structure and leaf properties. These are unknown in most remote sensing applications, but they can be retrieved by means of inverting a RTM using measured reflectance data (Houborg et al., 2007; Jacquemoud et al., 2009). The retrieved properties can then be used in a fluorescence RTM to quantify the SIF scattering. In this way, RTMs for reflectance and fluorescence can be used to interpret observed SIF signals.

Van der Tol et al. (2016) retrieved key biophysical and biochemical parameters from the reflectance data of rice canopies, and applied these parameters to simulate TOC SIF by using SCOPE. Such retrievals have a number of limitations. First, they are computational demanding. Second, both the retrieval of properties and prediction of SIF scattering are model dependent, and uncertainties in the estimation of canopy properties may be introduced due to ill-posed retrievals that may propagate into error in the prediction of canopy scattering of SIF. Nevertheless, Van der Tol et al. (2016) found that most of the variability of SIF could be reproduced after retrieval of parameters from reflectance. This not only confirms the dominating role of canopy scattering on seasonal variations of SIF, but also suggests that reflectance data can be used to estimate this scattering.

The idea that reflectance can explain the canopy scattering of SIF is promising. Reflectance data are widely available as many satellites have the capability to detect vegetation reflectance in many bands. The quantification of SIF scattering through reflectance measurements provides a way to decouple canopy structural and photosynthetic regulation effects on remotely sensed SIF.

Two recent studies provide experimental evidence of a close link between canopy scattering of SIF and reflectance. Badgley et al. (2017) reported that far-red reflectance times NDVI strongly correlates with SIF through the vegetated fraction of the surface. Liu et al. (2016) reported a bidirectional effect on SIF measurements that was similar to the effect on reflectance.

In the present study, we aim to link reflectance and canopy scattering of SIF by investigating the radiative transfer of incident light and emitted fluorescence with a minimum set of assumptions about the representation of canopies in models. We provide a detailed derivation of the canopy scattering of SIF and its relation to TOC reflectance. SCOPE model simulations are used to validate our findings. The relationship we found will allow rapid decoupling of canopy structural and functional regulation of SIF, which is useful for improving estimates of canopy photosynthesis from SIF.

2. Theoretical basis

2.1. Definitions and aim of study

The objective of the study is to relate the scattering of SIF (σ_{FC}) to TOC (directional) reflectance (R). R and σ_{FC} describe, respectively, the scattering of incident light and that of total emitted SIF to the viewing direction. They are defined as

$$R = \pi L_o / E \tag{1}$$

$$\sigma_{FC} = \pi L_o^F / E_F \tag{2}$$

where L_o and L_o^F are the radiance of observed reflected solar radiation and of observed fluorescence at top of canopy, respectively, and E and E_F are the irradiance of incident flux at top of canopy and emitted fluorescence from all the leaves in the canopy (i.e., fluorescence emission), respectively. Note that an observation is always the sum of L_o and L_o^F, and in remote sensing applications, they need to be separated with for example the FLD method (for a review, see Meroni et al., 2009). In radiative transfer modelling, they are separately simulated.

As mentioned, our objective is to express the canopy scattering of SIF σ_{FC} as a function of reflectance R:

$$\sigma_{FC} = f(R) \tag{3}$$

Reflectance and canopy scattering of SIF, and their relationship can be obtained if we know the observed radiance (L_o), observed fluorescence radiance (L_o^F), incident irradiance (E) and canopy total fluorescence emission (E_F). The incident irradiance is known in most cases either from measurements or from atmosphere radiative transfer models (e.g. MODTRAN, Berk et al., 2005), but E_F cannot be estimated easily.

In what follows, we derive an explicit expression of Eq. (3) in four steps, the final result of which is Eq. (12). First, we explain the interaction between incident flux and a vegetation canopy. Second, we provide an expression of canopy fluorescence emission. Third, we compare the equation for the observed reflected flux to that of the observed fluorescence flux. Finally, we link canopy scattering of SIF to TOC reflectance (Eq. (12)).

2.2. Flux interaction with vegetation canopy

Photons entering the canopy from the top will either go through the canopy via gaps or interact with leaves (or needles). The portion of photons from the incident beam that will not interact with leaves is known as the zero order transmittance (t_0). The complementary portion, the canopy interceptance (i_0), is the portion of photons that will interact with leaves (Smolander and Stenberg, 2005; Huang et al., 2007) (Fig. 1). The sum of the zero order transmittance and canopy interceptance is unity. The interception is the first order interactions between incident light and the canopy.

In the first order interactions, photons can either be scattered or absorbed by a leaf, depending on leaf albedo (ω), which is the sum of leaf reflectance (ρ) and transmittance (τ). Photons in the photosynthetically active radiation (PAR) range (i.e., from 400 to 750 nm)

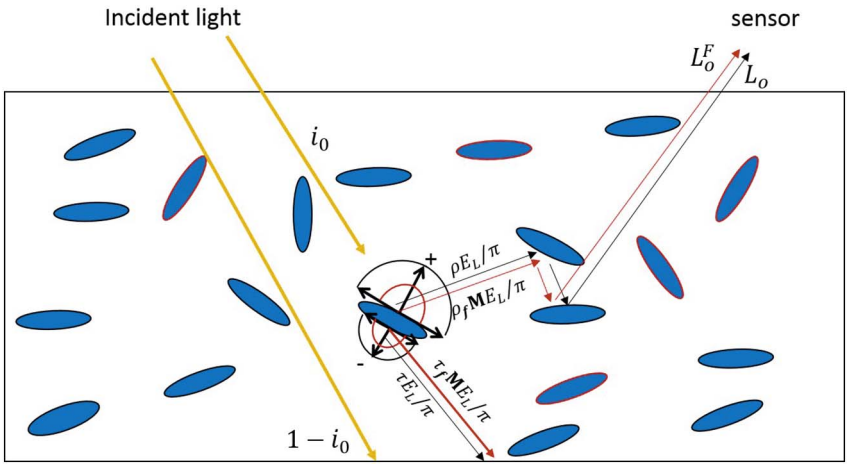

Fig. 1. The interaction between incident light and canopy. The ellipses represent leaves in the canopy, and red edges indicate the leaves are illuminated directly by the light from the top of the canopy. The fluorescence flux and scattered flux are represented by the red and black curves. The plus and minus signs indicate backward and forward sides of a leaf, respectively. (For interpretation of the references to colour in this figure legend, the reader is referred to the web version of this article.)

that hit the leaf, may also excite fluorescence photons in the wavelength range from 640 to 850 nm.

After the first order interactions, photons are scattered and fluorescence photons are emitted from the leaves that are illuminated directly by the (solar or diffuse) incoming light (Fig. 1). These photons interact with or escape from the canopy, and part of them will eventually be observed by a sensor at the top of canopy. The probability that photons will be observed, depends on the location of leaf, the direction of flux and wavelength of the photons, but it is independent of the origin of the photons (i.e., an emission or a scattering event). The equality of the radiative transfer of the scattered flux and emitted fluorescence after the first order interactions is the essence of the correlation between TOC reflectance and fluorescence scattering.

Fig. 2 summarizes the complete flux interactions with a canopy, starting from the first order interactions (in the middle of the figure). Emission and scattering events occur during the first order interactions (e1 and s1). Part of the scattered and emitted (fluorescence) photons may interact with the canopy for multiple times before escaping from the canopy. The multiple interactions can be divided into four classes: (1) scattered (fluorescence) photons are scattered again (s2), (2) emitted fluorescence photons are scattered (s3), (3) scattered photons excite fluorescence (e2), and (4) emitted fluorescence photons excite fluorescence (e3).

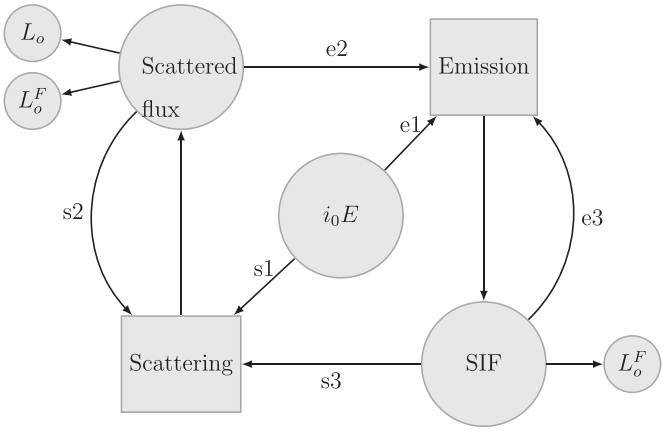

Fig. 2. Flux and vegetation canopy interaction diagram. The rectangles refer to scattering or fluorescence emission events. The circles refer to fluxes generated from the events. The arrows indicate changes of fluxes. E refers to the incident light. i_0 is the canopy interceptance, and thus i_0E is the light interacting with the canopy. i_0E will first be involved in scattering and emission events (s1 and e1), resulting scattered flux and SIF flux, respectively. Part of the fluxes will be observed fluxes by the sensor (L_o and L_o^F). The resulted scattered flux and SIF flux will be involved in scattering and emission events again (s2, s3, e2, e3), and further contribute to the observed fluxes.

The total fluorescence emission of the canopy is formed by all the interactions of PAR photons with the leaves (e1, e2 and e3). We found that for obtaining an explicit expression for $\sigma_{FC} = f(R)$, it is both necessary and justified to approximate that the canopy scattering of total emitted SIF (σ_{FC}) can be represented by the canopy scattering of SIF from the first order interactions (σ_{FC}^1), which means that excitation by scattered photons (e2) and excitation by fluorescence photons (e3) are not considered. The rationale for this assumption is twofold. First, most of the fluorescence is generated by sunlit leaves and shaded leaves exposed to the sky, which are both involved in the first order interactions. Second, the canopy scattering (i.e., a coefficient) of SIF from multiple interactions (e2, e3) (σ_{FC}^m) is comparable with, and therefore can be approximated by σ_{FC}^1. Further evidence justifying the approximation is provided in the Simulation results section.

2.3. Calculating fluorescence emission from the first order interactions

The fluorescence emission at a certain wavelength is excited by photons of different (i.e., shorter) wavelengths interacting with leaves. The relation between excitation of a leaf and emission of fluorescence is described by a so-called excitation-emission matrix, that quantifies the emission spectrum as a function of the excitation spectrum. This matrix depends on the radiative transfer within the leaf, and it can either be measured with dedicated equipments or simulated with leaf RTMs. In the model Fluspect (Vilfan et al., 2016), for example, the relationship between excitation and fluorescence emission is described by a 350 by 211 matrix $\mathbf{M}$ of 1 nm resolution values, with excitation wavelengths on rows and emission wavelengths on columns. The fluorescence emission from the first order interactions is expressed as

$$E_F(\lambda_f) = i_0 \int_{400}^{750} \mathbf{M}(\lambda_f, \lambda_e) E(\lambda_e) d\lambda_e = i_0 \mathbf{M} E \quad (4)$$

where $i_0E(\lambda_e)$ is the irradiance of PAR photons that are involved in the first order interactions, and $\mathbf{M}(\lambda_f,\lambda_e)$ is the excitation-emission matrix. The wavelengths of the excitation and fluorescence emission are λ_e ranging from 400 to 750 nm and λ_f ranging from 640 to 850 nm, respectively. Note that $\mathbf{M}\,E$ is matrix product that forms a vector. We take the inner product of one row of the matrix $\mathbf{M}$ with of the incident irradiance spectrum ($E_F(\lambda_f) = i_0\mathbf{M}\,E$) to describe the emission at a certain wavelength.

2.4. Observed flux and observed SIF flux

In order to calculate the canopy observed reflected flux and SIF flux, we first provide an expression for the fluxes originating from a single leaf, and then integrate the contributions of all the leaves over the canopy.

The incident radiation that hits a leaf $E_L(\lambda)$ depends on the location

of the leaf (x,y,z), leaf orientation (φ_l,θ_l), direction and intensity of the incident light (φ_l,θ_l), and is given as

$$E_L(\lambda) = P_s(x, y, z) f_s(\varphi_l, \theta_l, \varphi_s, \theta_s) E(\lambda) \quad (5)$$

where P_s is a boolean function that indicates whether the leaf is lit by the incident light directly ($P_s = 1$) or not ($P_s = 0$). The projection of a leaf into the direction of the incident light is established by f_s, which is a function of the azimuth (φ) and zenith (θ) angles of the leaf (l) and of the incident solar light (s) (Verhoef, 1984, 1985).

Assuming that both sides (i.e., the backward side and forward side) of the leaf are Lambertian, the fluxes from each side are isotropic. The photons emanating from the leaf thus consist of transmitted τE_L and reflected radiation ρE_L, backward emission $\rho_f \mathbf{M}\, E_L$ and forward emission $\tau_f \mathbf{M}\, E_L$, as shown in Fig. 1. The quantities ρ_f and τ_f describe the relative partitioning of the fluorescence emission over the backward and forward side, and the sum of them is unity in each wavelength (i.e., $\rho_f(\lambda) + \tau_f(\lambda) = 1$).

Part of the fluxes scattered from or emitted by the leaves during the first order interactions will be observed by the sensor at top of canopy. For one side of a leaf, the probabilities of the scattered fluxes and of the emitted fluxes from this side that will be observed by the sensor are the same. It is because that the probability that a photon from a leaf at location (x,y,z) will be observed depends on its wavelength and direction rather than its origin (i.e., emission event or scattered event). Therefore, the contribution of a leaf to the observed radiance and to observed fluorescence radiance can be expressed in a similar way.

$$\Delta L_o(\lambda) = \frac{E_L}{\pi}[\rho f_o(x, y, z, \lambda, \Omega_L \rightarrow \Omega_o) + \tau f_o(x, y, z, \lambda, -\Omega_L \rightarrow \Omega_o)] \quad (6)$$

$$\Delta L_o^F(\lambda) = \frac{\mathbf{M}E_L}{\pi}[\rho_f f_o(x, y, z, \lambda, \Omega_L \rightarrow \Omega_o) + \tau_f f_o(x, y, z, \lambda, -\Omega_L \rightarrow \Omega_o)] \quad (7)$$

where $f_o(x,y,z,\lambda,\Omega_L \rightarrow \Omega_o)$ and $f_o(x,y,z,\lambda,-\Omega_L \rightarrow \Omega_o)$ are the probability of observation of a flux from the leaf's backward and forward side, respectively. From hereon, they are represented by f_+ (backward) and f_- (forward) for convenience. The wavelength-dependence of the probabilities f_- and f_+ is due to the involvement of the wavelength-dependent multiple scattering.

The total observed radiance is the sum of the contributions of all the leaves in the canopy (assuming a non-reflecting background). After substituting E_L with Eq. (5), this sum is

$$L_o(\lambda) = \frac{E}{\pi} \sum_{leaves} [P_s f_s \rho f_+ + P_s f_s \tau f_-] \quad (8)$$

$$L_o^F(\lambda) = \frac{\mathbf{M}E}{\pi} \sum_{leaves} [P_s f_s \rho_f f_+ + P_s f_s \tau_f f_-] \quad (9)$$

2.5. Linking SIF scattering with reflectance

Using the observed radiances as in Eqs. (8) and (9), and incident irradiance E and SIF emission ($i_0\mathbf{M}\, E$, Eq. (4)), the reflectance and canopy scattering of SIF, as defined earlier in Eqs. (1) and (2) can be expressed as

$$R(\lambda) = \sum_{leaves} [P_s f_s \rho f_+ + P_s f_s \tau f_-] \quad (10)$$

$$\sigma_{FC}(\lambda) = \frac{1}{i_0} \sum_{leaves} [P_s f_s \rho_f f_+ + P_s f_s \tau_f f_-] \quad (11)$$

where the variables in front of and behind the plus signs represent contribution of backward and forward side to L_o or to L_o^F. It is noticed that both TOC reflectance and canopy scattering of SIF are a combination of $P_s f_s f_+$ and $P_s f_s f_-$. This provides the possibility to link them.

Finally, we are interested in the relationship between R and σ_{FC}. Although reflectance and canopy scattering of SIF are expressed similarly, the exact relation is still muddled. There is complexity in the seemingly simple Eqs. (10) and (11), caused by two facts: (1) A leaf does not scatter photons equally in both directions (forward and backward) and the probability of these photons emanating from these directions to reach the sensor is unequal, and (2) P_s, f_s, f_+ and f_- are different for each leaf, and different for different canopies. Therefore, the exact quantification of the relationship between σ_{FC} and R requires detailed radiative transfer modelling.

However, there are cases in which the relationship between σ_{FC} and R can be greatly simplified. First, if $f_+ = f_-$, using that $\omega = \rho + \tau$ and $1 = \rho_f + \tau_f$, we obtain

$$\sigma_{FC}(\lambda) = \frac{1}{i_0 \omega} R(\lambda) \quad (12)$$

Second, if the relative partitioning of the scattered radiation over the two sides of the leaves equals to the relative partitioning of the emitted fluorescence radiation over the two sides of the leaves, such that

$$\frac{\rho}{\tau} = \frac{\rho_f}{\tau_f}, \quad (13)$$

we also obtain the relationship as shown in Eq. (12) (i.e., from Eq. (13), we know that $\frac{\rho}{\rho_f} = \frac{\tau}{\tau_f} = \omega$).

In the far-red region (for the far-red SIF), the two conditions mentioned above are both reasonable, such that the relationship between σ_{FC} and R in Eq. (12) may exist. First, the difference between f_+ and f_- is smaller in the far-red region than in the red region. Emanating photons in this spectral region are normally involved in multiple interactions. With increasing interaction order, photons tend to 'forget' from which side of the leaf they originate (Mõttus and Stenberg, 2008). Second, Van Wittenberghe et al. (2015) compared the ratio of the backward and forward emission with the ratio of leaf reflectance and transmittance of a number of leaves from 4 species. They found a linear relationship between $\frac{\rho}{\tau}$ and $\frac{\rho_f}{\tau_f}$ in the far-red region. These two arguments strongly support the validity of the relationship in Eq. (12) in the far-red region.

On the contrary, the two conditions mentioned above may not be true in the red region (for the red SIF). First, the contribution of photons from the first order interactions in the red region to L_o or L_o^F is mainly from direct observation instead of observation after multiple interactions. As a result, the difference between f_+ and f_- caused by the different origins (i.e., backward or forward side) is more in the red than in the far-red region. Second, an exponential decay function between $\frac{\tau_f}{\rho_f}$ and $\frac{1}{\tau}$ was found in the red region (Van Wittenberghe et al., 2015). In fact, the ratios on both sides of Eq. (13) are very sensitive to pigment pool of the leaf in the red region. The validity of neither the condition in Eq. (13) nor the condition that $f_+ = f_-$ is guaranteed in the red region. Therefore, the relationship between σ_{FC} and R of Eq. (12) may not hold for red SIF.

3. SCOPE simulation method

We tested the relationship between canopy scattering of SIF (σ_{FC}) and TOC reflectance (R) as shown in Eq. (12) by using simulations with the SCOPE model (Van der Tol et al., 2009) for a number of scenarios. Several assumptions were also tested by using SCOPE simulations. In total, 1800 scenarios of combinations of different leaf properties, canopy structure or sun zenith angles were generated.

We first studied the spectra of canopy scattering of SIF (σ_{FC}) and tested the sensitivity to changing of LAI and leaf chlorophyll content, which are two key canopy properties. Further, we focused on the results for canopy scattering of SIF at 687 nm and 760 nm (F_{687} and F_{760}), representing the red and far-red fluorescence used in remote sensing of vegetation (Meroni et al., 2009).

3.1. SCOPE model

SCOPE is a model for homogeneous vegetation and consists of a leaf RTM, several canopy RTMs and an energy balance model. At the leaf level, Fluspect (Vilfan et al., 2016), which is based on PROSPECT (Jacquemoud and Baret, 1990), simulates leaf reflectance (ρ), transmittance (τ), and fluorescence emission of the both forward and backward side. At the canopy level, RTMo and RTMf, which are two SAIL (Verhoef, 1984) based models, compute the radiative transfer of incident radiation and emitted fluorescence, respectively.

SCOPE provides the necessary output to test the relationship we found. TOC reflectance (R) and fluorescence (L_o^F) are two direct outputs of SCOPE. Canopy fluorescence emission (E_F) is computed by SCOPE, but it is not stored as output. We modified SCOPE version 1.70 to store it as output. We computed the canopy scattering of SIF for each scenario according to Eq. (2). Canopy interceptance (i_0) is a spectral invariant determined by canopy LAI and leaf inclination distribution (Smolander and Stenberg, 2005). The literature about the spectral invariant theory provides equations for i_0 (e.g., Smolander and Stenberg, 2005; Huang et al., 2007). In SCOPE, it is calculated as $1 - \exp(-kL)$, where k is the extinction coefficient and L is canopy leaf area index. The extinction coefficient is determined by sun zenith angle and leaf inclination distribution. We used the canopy interception as simulated by SCOPE, and modified the code to save it as output. For leaf albedo, we used the sum of leaf reflectance and transmittance as simulated by Fluspect.

3.2. Database generation

The input of SCOPE for the 1800 scenarios comprises of 60 combinations of leaf properties, 10 combinations of canopy structure parameters, and 3 sun zenith angles (Table 1). The values of parameters for leaf properties, canopy structure and sun position were chosen within the recommended ranges in SCOPE (Van der Tol et al., 2009; Yang et al., 2017) with non-linear steps. The viewing zenith angle was 0° (i.e. at nadir), and a non-reflecting background and a typical incident irradiance spectrum were used (i.e., default setting in the SCOPE model, see Supplementary materials).

TOC reflectance, TOC SIF, and total SIF emission of the 1800 scenarios were simulated with SCOPE. Leaf reflectance (ρ), transmittance (τ), fluorescence emission on the backward and forward side, and thus ρ_f and τ_f were simulated for the 60 leaves.

3.3. Testing the assumptions

The assumption that the canopy scattering of SIF (σ_{FC}) can be approximated by scattering of SIF from the first order interactions (σ_{FC}^1) was tested by using SCOPE simulations. We also compared $\frac{\rho}{\tau}$ and $\frac{\rho_f}{\tau_f}$ from Fluspect simulations.

To test the two statements in Section 2.2 that 1) the observed SIF from canopy scattering is most from the first order interactions, and 2) scattering of SIF from first order interactions (σ_{FC}^1) and multiple interaction (σ_{FC}^m) are comparable, two sets of simulations were conducted. In these simulations, SIF emission from the first order interactions (E_F^1) and from the multiple interactions (E_F^m) of the 1800 scenarios were separately simulated as well as the correspondingly observed SIF (L_o^{F1} and L_o^{Fm}) and scattering coefficients (σ_{FC}^1 and σ_{FC}^m). This was done by modifying the input to RTMf in the code of SCOPE, notably by removing the scattered light and the direct incident light distributed in the canopies in RTMf, respectively. The light distribution inside the canopy was simulated in RTMo and later used as input of RTMf for fluorescence simulations. SIF emission during the first order interactions was excited by the direct solar flux (i.e., we used the direct solar beam as incident light). Therefore, by removing the scattered light in the input of RTMf, we obtained SIF emission from the first order interactions, and the corresponding SIF observed at top of canopy and thus computed σ_{FC}^1. Conversely, SIF emission from the multiple interaction was excited by the scattered light. By removing direct light distributed in the canopy in RTMf, we obtained E_F^m, L_o^{Fm} and σ_{FC}^m. We compared the canopy SIF emission from the first order interactions and from the multiple interactions of the scenarios as well as TOC SIF observed as simulated with SCOPE. Further, σ_{FC}^1 and σ_{FC}^m were compared. The simulated results of the 1800 scenarios were grouped by canopy LAI. There were 360 simulations for each unique LAI value. The mean and standard derivation of each group were computed and compared. It should be noted that SCOPE simulates fluorescence excited by scattered photons (e2 in Fig. 2), but it neglects the much smaller flux of fluorescence excited by fluorescence photons (e3).

To test the condition that $\frac{\rho}{\tau} = \frac{\rho_f}{\tau_f}$ in Section 2.4, we compared the two ratios simulated from Fluspect for the 60 leaves comprising all the combinations of the leaf parameters in Table 1. Leaf reflectance and transmittance were direct outputs of Fluspect, and $\frac{\rho_f}{\tau_f}$ were computed as the ratio between backward and forward fluorescence emission of the leaves.

Table 1
Summary of SCOPE inputs applied for the generation of the database.

Parameter	Explanation	Unit	Values
C_{ab}	Chlorophyll $a + b$ content	μg cm^{-2}	5, 10, 20, 40, 80
C_{dm}	Leaf mass per unit area	g cm^{-2}	0.01, 0.02
C_w	Equivalent water thickness	cm	0.015, 0.03
N	Leaf structure parameter	–	1, 1.5, 2
LAI	Leaf area index	–	0.5, 1, 2, 3, 6
LIDFa	Leaf inclination function parameter a	–	− 0.5, 0.5
θ_s	Sun zenith angle	°	30, 45, 60

3.4. Validation of the relationship between reflectance and canopy scattering of SIF

To test whether $\frac{\rho}{\tau} = \frac{\rho_f}{\tau_f}$ (Eq. (13)) is a sufficient condition of the relationship between σ_{FC} and R in Eq. (12), two types of simulations were carried out, each consisting of the 1800 scenarios described above (3600 simulations in total). In the first group of 1800 simulations (group-1), we modified the Fluspect output of the 60 leaves in such a way that the assumption in Eq. (13) was fulfilled. The leaf albedo of the 60 leaves was calculated as the sum of reflectance and transmittance, and likewise, fluorescence emission was calculated as the sum of the forward and the backward emission. Leaf reflectance and transmittance were then recalculated as $\omega/2$ each, and likewise, forward and backward fluorescence as half of the total fluorescence each (i.e., $\rho = \tau = \omega_L/2$ and $\rho_f = \tau_f = 0.5$). Note that taking equal ρ and τ, and ρ_f and τ_f is a special case among all cases that comply with Eq. (13). These leaves are considered as synthetic leaves. In the second group of simulations (group-2), the manipulations above was not carried out, and leaf reflectance and transmittance, and forward and backward emission as simulated by Fluspect were used directly. These leaves are considered as Fluspect leaves.

We validated the relationship of canopy SIF scattering and reflectance in Eq. (12) for both red and far-red SIF. Both the group-1 and group-2 simulations from SCOPE were used to evaluate the relationship.

4. Simulation results

4.1. Canopy scattering of SIF

The canopy scattering of SIF (σ_{FC}) was spectrally dependent (Fig. 3). The value of σ_{FC} was much higher in the near-infrared region than in the red region. Furthermore, it increased with LAI in the near-infrared region, but decreased in the red region.

Leaf chlorophyll content strongly affected σ_{FC} in the red region, but

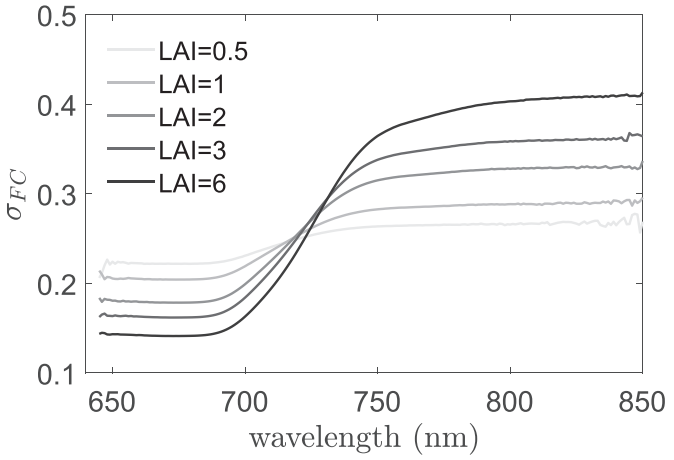

Fig. 3. The canopy scattering of SIF (σ_{FC}) in the spectral region from 640 nm to 850 nm simulated by using SCOPE. In the simulations, LAI was set to 0.5, 1, 2, 3 or 6. Leaf chlorophyll C_{ab} = 40 μg cm^{-2}. Leaf structure parameter N = 1.5. Leaf mass C_{dm} = 0.01 g cm^{-2}. Equivalent water thickness C_w = 0.015 cm. LIDFa = − 0.5. Sun zenith angle θ_s = 30°.

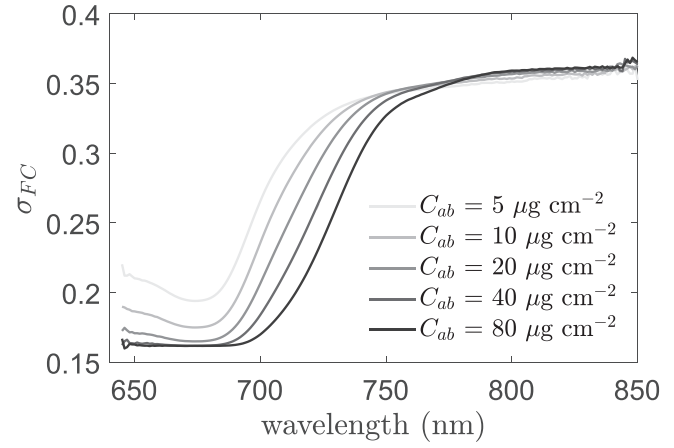

Fig. 4. The canopy scattering of SIF (σ_{FC}) in the spectral region from 640 nm to 850 nm simulated by using SCOPE. In the simulations, leaf chlorophyll C_{ab} was set to 5, 10, 20, 40 or 80 μg cm^{-2}. LAI = 3. Leaf structure parameter N = 1.5. Leaf mass C_{dm} = 0.01 g cm^{-2}. Equivalent water thickness C_w = 0.015 cm. LIDFa = − 0.5. Sun zenith angle θ_s = 30°.

had almost no impact on σ_{FC} in the near-infrared region (Fig. 4). The higher leaf chlorophyll content resulted in lower σ_{FC} in the red region.

4.2. SIF from first order and multiple interactions

Fig. 5 shows that the SIF emission from the first order interactions between the incident light and canopies was much higher than SIF emission from the multiple interactions (i.e., emitted by scattered PAR photons) at both 687 nm and 760 nm. SIF observed at the top of the canopies was also mostly from the first order interactions at both 687 nm and 760 nm (Fig. 6). Both canopy emitted SIF and observed SIF increased with the increasing LAI at both 687 nm and 760 nm.

The scattering of whole canopy SIF (σ_{FC}) closely matched with the scattering of SIF from the first order interactions alone (σ^1_{FC}) (Fig. 7). The difference between σ^1_{FC} and σ^m_{FC} was less than 30%. Canopy scattering of far-red SIF increased but that of red SIF decreased with LAI as also shown in Fig. 3.

4.3. Radiation distribution over two sides of leaves

The distributions of scattered and emitted photons over the two sides of the leaf as simulated with Fluspect were similar in the far-red spectral region, but this symmetry was much less for red region (Fig. 8). Both ρ/τ and ρ_f/τ_f were sensitive to leaf structure (N) at 760 nm. The pigments content had no impact on ρ/τ at 760 nm. On the contrary, the two quantifies at 687 nm were sensitive to both leaf structure and pigments content.

4.4. Relationship between TOC reflectance and canopy scattering of SIF

Fig. 9 shows that σ_{FC} predicted from canopy reflectance (i.e., $\sigma_{FC} = \frac{R}{i_0\omega}$) from the group-1 simulations was in almost perfect agreement with σ_{FC} simulated with SCOPE at both 687 nm and 760 nm, with both R^2 = 0.98. Small excursions from 1-1 line were found in only few of the 1800 scenarios.

Fig. 10 shows that the correlation between σ_{FC} and $\frac{R}{i_0\omega}$ was stronger for 760 nm than for 687 nm when the Fluspect leaves were used (group-2 scenarios). For the far-red SIF (F_{760}), σ_{FC} and $\frac{R}{i_0\omega}$ showed significant positive correlation with R^2 = 0.772. This was obviously lower than for group-1 simulations, but still significant. The correlation was poor for red SIF (F_{687}). Although σ_{FC} and $\frac{R}{i_0\omega}$ were still positively correlated, the excursions from the 1:1 line were substantial in many scenarios. However, for a individual leaf, σ_{FC} and $\frac{R}{i_0\omega}$ were also linear when canopy structure (LAI and LIDFa), and sun zenith angle were changing. The slope of the relationship between σ_{FC} and $\frac{R}{i_0\omega}$ was leaf dependent. In Fig. 10, we only randomly marked three individual leaves for readability of the figure (for the correlation of individual leaves, see the Supplementary material).

5. Discussion

5.1. Interpretation by using spectral invariant theory

The analogy of radiative transfer of intercepted incident light and emitted SIF allowed us to derive the relationship between reflectance (R) and canopy scattering of SIF (σ_{FC}), merely by reasoning rather than detailed modelling. The relation in Eq. (12) can also be obtained from existing spectral invariant recollision theory, as follows.

Smolander and Stenberg (2005) introduced the recollision probability p to calculate total scattering $s(\lambda)$ of a canopy (bounded underneath by a non-reflecting surface)

$$s(\lambda) = i_0 \frac{(1-p)\omega(\lambda)}{1-p\omega(\lambda)} \tag{14}$$

where the recollision probability p is defined as the probability that a photon, after having survived an interaction with a canopy element, will interact with the canopy again.

A second spectral invariant, the directional escape probability $\rho(\Omega)$, quantifies the portion of scattered photons that escapes via gaps in the direction of viewing (Huang et al., 2007). Canopy directional reflectance can be expressed as (Schull et al., 2007; Köhler et al., 2018)

$$R = i_0\rho(\Omega)\frac{\omega(\lambda)}{1-p\omega(\lambda)} \tag{15}$$

Canopy scattering of SIF can be expressed by using the spectral invariants as well. A TOC SIF observation includes contributions from a series of progressively smaller components: 1) emitted SIF photons that directly escape and are observed by the sensor ($\rho(\Omega)$); 2) emitted SIF photons that interact once with the canopy before escaping and being observed ($p\omega(\lambda)\rho(\Omega)$); 3) emitted SIF photons that interact twice before escaping and being observed ($p^2\omega(\lambda)^2\rho(\Omega)$), etc. The total canopy scattering of SIF is the sum of the contributions, which is given as a geometric series:

$$\sigma_{FC}(\lambda) = \rho(\Omega) + p\omega(\lambda)\rho(\Omega) + p^2\omega(\lambda)^2\rho(\Omega) + \ldots = \frac{\rho(\Omega)}{1-p\omega(\lambda)} \tag{16}$$

Note that both $\rho(\Omega)$ and p are spectral invariant and depend on

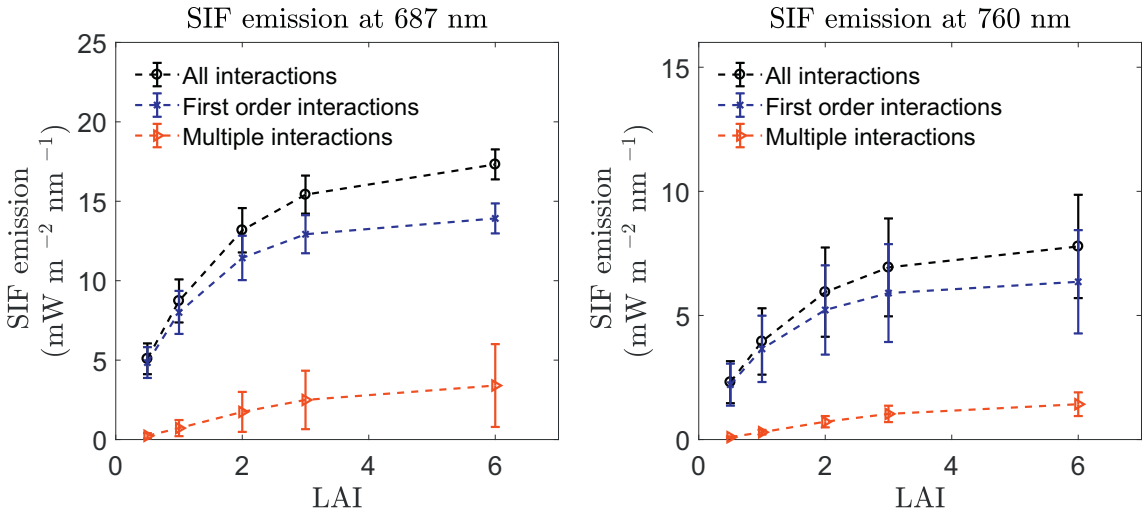

Fig. 5. SIF emission at 687 nm and 760 nm from all the interactions, the first order interactions and multiple interactions changing with LAI. The error bars represent the total range of variation of the 360 scenarios with the same LAI but different leaf properties, leaf orientations or sun zenith angles. Note: SIF from the first order interactions refers to the fluorescence emission by incident light directly. SIF from the multiple interactions is the fluorescence emission excited by scattered light.

canopy structure. Dividing Eq. (16) by Eq. (15) eliminates ρ(Ω) and p, and results in Eq. (12).

Eq. (12) can thus be obtained from spectral invariant theory as well, but the theoretic derivation in Section 2 is more general. In the spectral invariant theory, leaf single scattering is quantified by leaf albedo (ρ + τ), while ρ and τ are not considered separately. However, the difference ρ − τ appears to be essential: The asymmetry of leaf scattering explains why the simple relationship between TOC reflectance and scattering of SIF is valid for the far-red region, but not for red region.

The canopy scattering of SIF is also linked with the directional area scattering factor (DASF) (Knyazikhin et al., 2013), which is a combination of the three spectrally invariant parameters (i.e., i_0, p and ρ).

$$\mathrm{DASF} = \frac{\rho(\Omega) i_0}{1 - p} \tag{17}$$

DASF is the TOC directional reflectance if the foliage does not absorb radiation (i.e., $\omega = 1$). At weakly absorbing wavelengths, for example, in near-infrared region, σ_{FC} can be approximated by DASF/i_0 or by R/i_0 (i.e., DASF = R, when $\omega = 1$).

5.2. Canopy scattering of SIF and reflectance

Canopy scattering of SIF and reflectance are affected by leaf properties and canopy structure in a comparable way. The content of pigments in a leaf mostly affects σ_{FC} in the red region, but not in the near-infrared region. For example, σ_{FC} in the near-infrared region does not change with leaf chlorophyll content (Fig. 4). Likewise, near-infrared reflectance is not sensitive to leaf chlorophyll content (Jacquemoud et al., 2009). Both σ_{FC} (Fig. 2) and R (Jacquemoud et al., 2009) respond to canopy LAI differently in the red and near-infrared region: they increase with LAI in the near-infrared region, but decrease in the red region. For the red SIF, the signal at top of canopy is mainly from the emitted SIF from leaves that are directly observed via gaps. The contribution from emitted SIF after interacting with leaves again is rather small. Higher LAI normally associates with lower canopy gap fraction. Therefore, a smaller portion of the emitted SIF will be observed, and thus a smaller σ_{FC}. On the contrary, far-red SIF is strongly affected by multiple scattering, which increases with LAI.

The sensitivity of σ_{FC} and R to canopy structure and leaf properties is, however, not exactly the same. σ_{FC} is mostly determined by the canopy gap fraction, while TOC reflectance is determined jointly by the

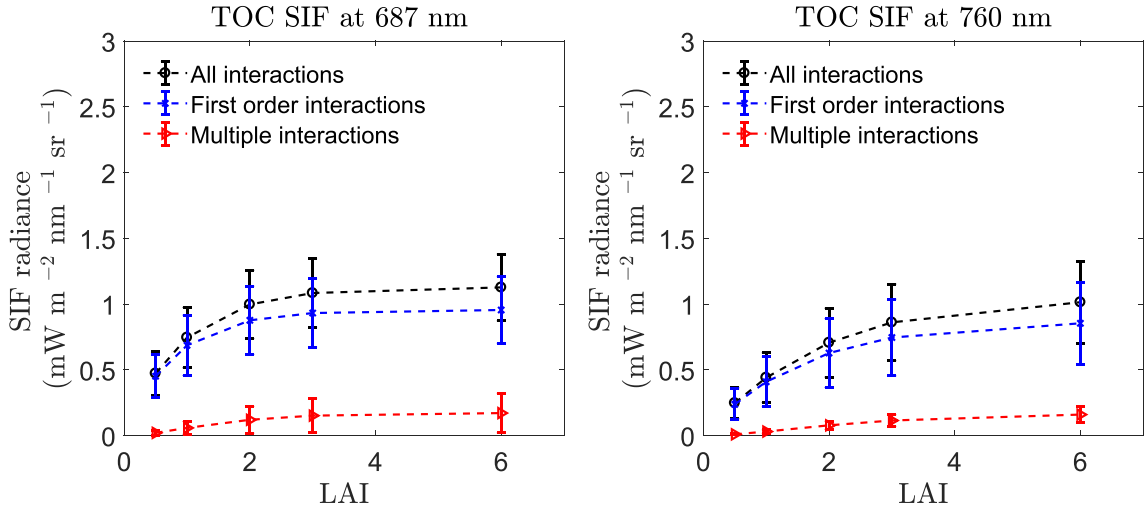

Fig. 6. Radiance of top-of-canopy (TOC) SIF observed at 687 nm and 760 nm from all the interactions, the first order interactions and multiple interactions changing with LAI.

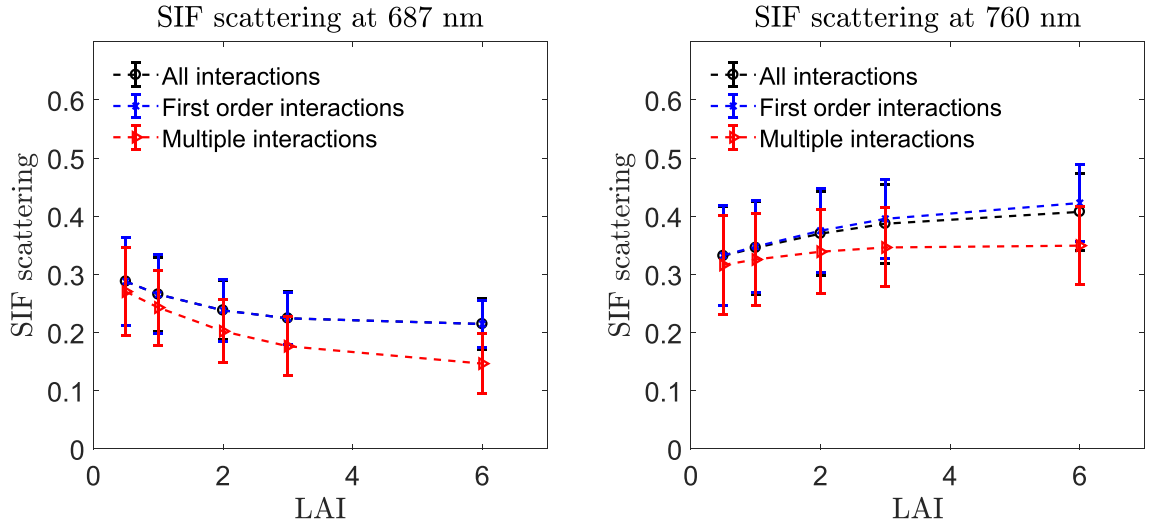

Fig. 7. Canopy scattering of SIF at 687 nm and 760 nm from all the interactions, the first order interactions and multiple interactions changing with LAI.

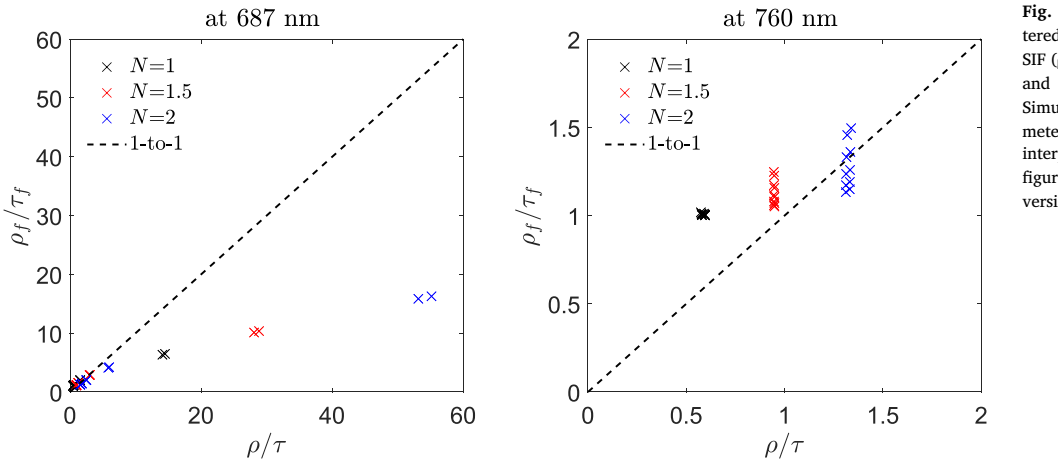

Fig. 8. The comparison of partitioning of scattered radiation (ρ/τ) and partitioning of emitted SIF (ρ_f/τ_f) over the two sides of leaves at 687 nm and 760 nm simulated with Fluspect. Simulations with the same leaf structure parameter (N) are marked with the same colour. (For interpretation of the references to colour in this figure legend, the reader is referred to the web version of this article.)

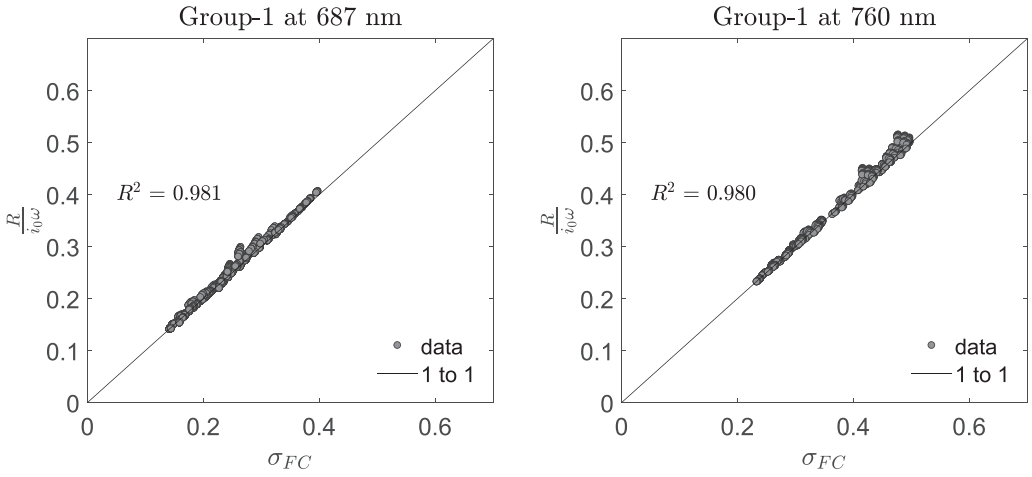

Fig. 9. The correlation between canopy scattering of SIF (σ_{FC}) and $\frac{R}{i_0\omega}$ at 687 nm and 760 nm for the group-1 (synthetic leaves) scenarios. Each point represents one scenario. Every leaf in the group had equal reflectance and transmittance ($\rho = \tau = \omega/2$), and equal backward and forward fluorescence emission. Note: R is canopy reflectance, i_0 is the canopy interceptance and ω is the leaf albedo.

light interception (i_0) and gap fraction. A lower canopy fraction results in a higher observation probability of the emitted fluorescence, but it also results in a lower i_0. The lower i_0 and higher gap fraction have an opposite (i.e. cancelling) effect on the TOC red reflectance. As a consequence, the red reflectance is less sensitive to LAI than the scattering of red SIF (compare Fig. 3 to Fig. 3 in Jacquemoud et al. (2009) or to Fig. 2d in Jacquemoud (1993)).

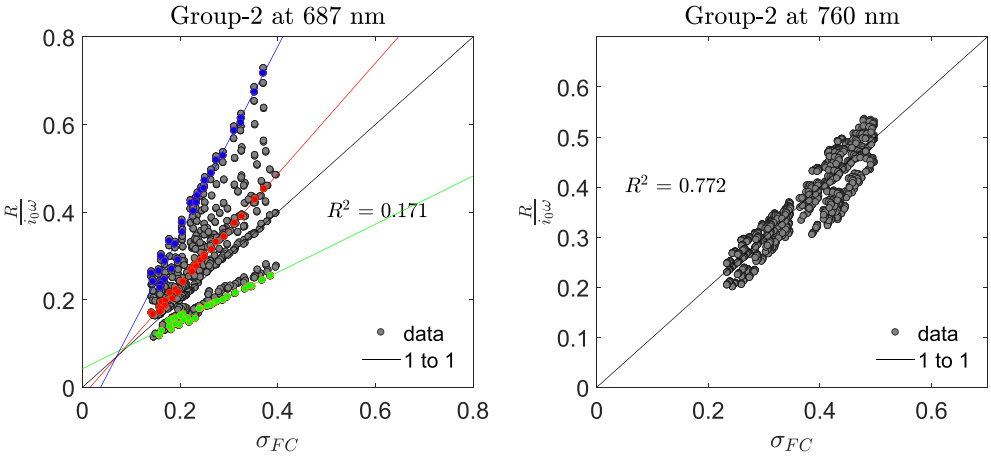

Fig. 10. The correlation between canopy scattering of SIF (σ_{FC}) and $\frac{R}{i_0\omega}$ at 687 nm and 760 nm for the group-2 (Fluspect leaves) scenarios. Each point represents one scenario. Simulations of scenarios that have the same leaf are highlighted with the same colour. Three individual leaves are respectively marked as red, blue and green for illustration, while the remaining 57 leaves are marked as gray. Note: R is canopy reflectance, i_0 is the canopy interceptance and ω is the leaf albedo. (For interpretation of the references to colour in this figure legend, the reader is referred to the web version of this article.)

5.3. Validity of the relationship between canopy scattering of SIF and reflectance

The relationship between σ_{FC} and TOC reflectance relies on the analogy of radiative transfer of intercepted incident light and emitted SIF. It has a physical basis. In our derivation, it is important to separate the first order interactions and multiple interactions. The first order interactions are the interception of incident light, which results in the scattered radiation and fluorescence emission. Further scattering by subsequent interactions determines the probability that the photons resulting from the first order interactions can be observed at the top of canopy from a specific direction. This further scattering is indifferent to the source of the photons (i.e. scattering or emission), and this is the basis for the relationship between SIF scattering and reflectance, namely that the scattering of SIF is proportional to the ratio of reflectance to the product of the canopy interceptance and the leaf albedo ($R = i_0\omega\sigma_{FC}$).

Several assumptions underlay our derivation. In deriving the equations for reflectance and SIF scattering (Eqs. (10) and (11)), we neglected two sources of fluorescence produced in higher order interactions, notably the excitation of fluorescence by scattered light and the excitation of fluorescence by fluorescence photons (e2 and e3 in Fig. 2). This simplification appears to be justified: the scattering of SIF as simulated by SCOPE matches closely with the scattering of SIF from the first order interactions (σ^1_{FC}) (Fig. 7). Although SCOPE also neglects the (very small) flux of excitation of fluorescence by fluorescence photons (e3), it does account for the excitation of fluorescence by scattered light (e2). In the development and validation of the relationship, we did not consider the effects of a non-fluorescent soil background. In evaluating of the effect of the soil, we need to differentiate between direct and scattered radiation (i.e. after at least one interaction) reaching the soil. The latter does not affect the relationship we found, because the scattering of the soil is indifferent to the source (emitted SIF or scattered incident), and these effects are included in f_+ and f_-. However, the part of the soil receiving solar or sky light directly, can contribute to the observed reflected flux, but not to the observed SIF because it does not produce SIF. The direct contribution of sunlit soil to TOC reflectance (Eq. (10)) can be expressed as $(1 - i_0)r_sP_o$, where $(1 - i_0)$ is the probability of photons to exit the canopy directly (zero order transmittance, t_0), r_s is soil reflectance and P_o is the probability that the soil will be observed. This contribution may affect the relationship and change with canopy coverage, but quantification of the exact impact requires further investigation.

More critical is the directionality (i.e., forward or backward) of the fluxes generated by leaves in the first order interactions. If the distribution of scattered light over reflection and transmission is different from the distribution of emitted fluorescence over the two sides of the leaf, then our simplified relation of Eq. (12) does not hold, because forward and backward propagated light scatter differently in subsequent interactions. In that case, no simple mathematical expression can describe the relationship between fluorescence scattering and reflectance. The asymmetry between the distribution of scattered and emitted photons over the two sides of the leaf, combined with the fact that the canopy scattering f_- and f_+ are unequal in the red region, make the relationship between canopy scattering of fluorescence and reflectance deviate from the general form of Eq. (12). This relation is leaf property dependent in the red region and may depend on the arrangement of pigments in the leaf (Vogelmann and Han, 2000).

Interestingly, $\frac{R}{i_0\omega}$ and σ_{FC} are still proportional in the red (but not equal) for individual leaves in the 30 simulated canopies, but the slope of the relationship varies with leaf structure and pigment composition (see Supplementary information). A more general expression for the scattering of fluorescence in the red region would require the inclusion of scattering within the leaf in the analysis, which would be an extremely useful line to investigate further.

In the derivation of Eq. (12), we did not parameterize the structure of the canopy (such as leaf shape and leaf inclination distribution, fractional cover), and thus, did not make assumptions on the form and representation of the canopy in a model. This makes our results generic, and Eq. (12) should be applicable to a wide range of canopies. For the validation of the equation, we used a turbid canopy model (SCOPE) in which P_s, f_s, f_+ and f_- are functions of the vertical position of the leaf in the canopy (in units of LAI), but are independent to the horizontal position (x,y), but the applicability of Eq. (12) is not limited to canopies that can be considered as a turbid medium. The fact that the same relationship can be derived using spectral invariant theory supports the potential application in needle forest (Rautiainen and Stenberg, 2005) and clumped canopies (Stenberg and Manninen, 2015). We even expect that the relationship is more promising for needle forest, since the asymmetry in needles is less obvious than in leaves. However, the general relationship of Eq. (12) relies on the assumption that leaves have equal properties in the whole canopy. Although this is a common assumption in many radiative transfer models, it could be relaxed in some detailed radiative transfer models for further testing of the relationship between SIF scattering and reflectance.

5.4. Validation of the relationship

Direct validation of the relationship in Eq. (12) requires the measurements of TOC reflectance, canopy interceptance, leaf albedo and canopy scattering of SIF. The last one (σ_{FC}) can be computed knowing the total emitted SIF of the canopy and TOC SIF observed. Canopy SIF measurements are retrieved from various platforms by using the FLD methods. It is also possible to measure total emission by using some dedicated instruments, such as FluoWAT (Van Wittenberghe et al., 2012; Cendrero-Mateo et al., 2015), but a representative number of leaves needs to be measured. Besides of the labor consuming, the requirement of simultaneous measurements of leaf SIF and canopy SIF makes the direct validation difficult.

Indirect validation by looking into the directional effects on SIF and reflectance is more practical. According to the relationship we found, the viewing angle effects on TOC SIF and reflectance are analogous. SIF observed from different angles differs from each other due to the different canopy scattering of the emitted SIF. The variation in view angles does not affect the total emission, but only the canopy scattering of SIF which is linked with reflectance (Eq. (12)). Field measurements presented in Liu et al. (2016) provides evidence for the similar viewing angle effects on SIF and on reflectance. A demonstrative simulation with SCOPE confirms the identical viewing zenith angle effects on SIF and on reflectance, at both 687 nm and 760 nm (Fig. 11). A recent study by Köhler et al. (2018) also reported a similar albeit not identical directional effect of geometry on GOME-2 far-red SIF and near-infrared reflectance. The effects were not identical due to variations in incident light intensity caused by variations in solar angle. In Köhler et al. (2018) study, both solar angle and viewing angle varied (i.e., their changes were quantified by the phase angle). In contrast to viewing angle, the effect of solar zenith angle is not identical for reflectance and SIF. The solar zenith angle affects the incident light intensity and the canopy interception of the incident light (i_0), and thus SIF emission. Therefore, the sun zenith angle affects the slope of SIF versus reflectance relationship via the incident light intensity, according to Eqs. (12) and (2).

The SCOPE simulations and the spectral invariant theory support the relationship we derived. The relationship between σ_{FC} and R was developed analytically in Section 2, and confirmed by SCOPE simulations. SCOPE has a fundamentally different basis of radiative transfer compared to the theory presented in Section 2. In the simulations, a wide range of scenarios were tested, including various canopy structure, leaf properties and sun zenith angles. Obviously, the validation is limited for canopies that can be represented by SCOPE, but the presented relationship is more general. Furthermore, the alternative approach to derive Eq. (12) by means of the widely used spectral invariant theory contributes to the confidence in our derivation.

5.5. Implications for remote sensing

The presented relationship between canopy scattering of SIF and reflectance has potential applications in remote sensing. The relationship we found can be used to correct the directional effect on SIF. Eq. (12) explains the similarity of the directional effects of SIF and of reflectance. The proportionality between R and σ_{FC} with the ratio (i.e., $i_0\omega$ in the far-red region) that is independent to view angles results the same directional effects of SIF and reflectance. Normalizing TOC SIF by reflectance may be an approach to correcting the viewing angle effects on SIF.

Eq. (12) also makes it possible to estimate the total emitted SIF using directional measured SIF and reflectance. A requirement is that the canopy interceptance and the leaf albedo are known. Canopy interceptance is a widely used spectral invariant that only depends on the canopy structure and sun position (Huang et al., 2007; Smolander and Stenberg, 2005). It can either be computed giving the canopy structure and sun zenith angle (Stenberg and Manninen, 2015), or estimated from canopy reflectance (Asrar et al., 1986; Bartlett et al., 1989). Leaf albedo in the far-red region is close to unity due to the strong scattering within the leaf. Nevertheless, it is necessary to estimate its value in order to apply Eq. (12), which means that inverse radiative transfer modelling may still be required in order to obtain ω. Once ω and i_0 are known, canopy scattering of far-red SIF can be estimated from reflectance data, and the canopy structural and functional regulation on far-red SIF decoupled. Several studies interpret SIF observation from satellite by normalizing the cosine of solar zenith angle as a better indicator of plant physiology changes (Frankenberg et al., 2011; Joiner et al., 2011). This normalization accounts for the solar zenith angle dependence of the incoming solar irradiance, but does not account for spatial or temporal variations in fraction of absorbed PAR (FAPAR) and σ_{FC} (Joiner et al., 2011). Cosine of solar zenith angle is related to i_0 (Stenberg and Manninen, 2015). Normalizing TOC SIF by cosine of solar zenith angle and TOC reflectance may partially correct the variation of σ_{FC}.

It is promising to consider the canopy structure effects on FAPAR together with σ_{FC}. Canopy structure effects on SIF observations include the impact on the process of light absorption and the process of scattering of emitted SIF. By 'removing' these effects from the observed SIF, we are able to estimate the fluorescence emission efficiency, which is a 'pure' functional trait directly linked to photosynthetic efficiency. The fluorescence emission efficiency can be computed as the normalization

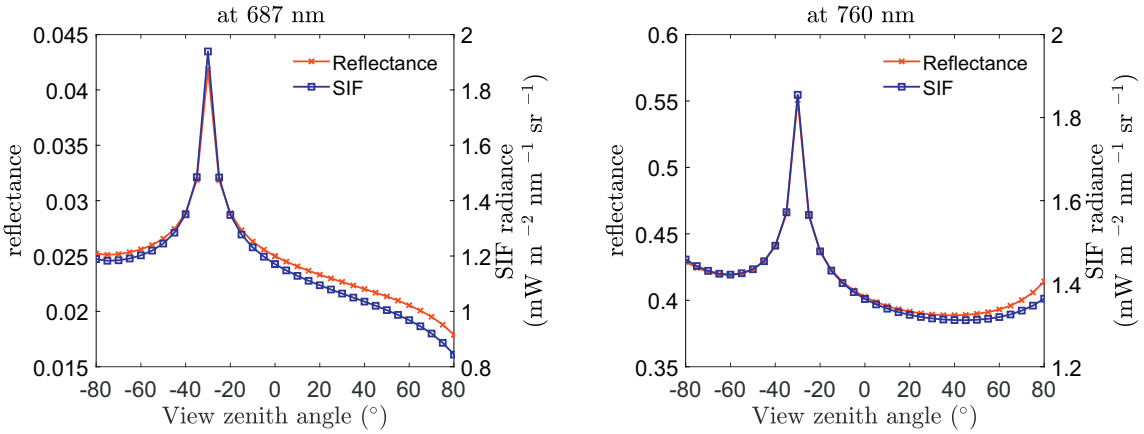

Fig. 11. View zenith angle (VZA) effects on reflectance and SIF at 687 nm and 760 nm simulated with SCOPE. Negative values of the VZA represent the backward direction, and positive values represent the forward direction. The key model parameters were set as follows: sun zenith angle θ_s = 30°, relative azimuth angle between sun and view Ψ = 0°, chlorophyll content C_{ab} = 40 μg cm^{-2}, leaf structure parameters N = 1.5, LAI = 3, leaf inclination parameters LIDFa = 0.5 and LIDFb = 0.5.

of SIF by the product of σ_{FC} and absorbed PAR. In this study, we propose an approach for estimating canopy scattering of SIF from TOC reflectance, canopy interceptance and leaf albedo. The fraction of absorbed PAR can be also estimated by using leaf albedo and spectral invariants (Fan et al., 2014). Considering absorption of incident light and scattering of emitted light together, we may quantify the total effects of canopy structure on SIF observations only by using TOC reflectance.

6. Conclusion

Separation of canopy structural and photosynthesis functional regulation on SIF observations is crucial for estimating photosynthesis from SIF. The analogy of the radiative transfer of emitted SIF and intercepted incident light allows linking canopy scattering of SIF to reflectance observations. By comparing their radiative transfer, a theoretical relationship between reflectance and canopy scattering of SIF was found: Canopy scattering of far-red SIF can be expressed as a simple function of canopy interceptance, TOC reflectance and leaf albedo. The equation is valid if the directionality of leaf fluorescence emission is similar to the directionality of leaf scattering, a condition that is met in the far-red region, but not in the red region of the electromagnetic spectrum. The relationship we presented provides an easy and accurate approach for decoupling the canopy structural and directional effects on far-red SIF measurements. The relationship between canopy scattering of SIF and reflectance explicates that reflectance and SIF observations combined can provide a diagnose of photosynthetic functioning.

Acknowledgments

This work of the first author (Peiqi Yang) was supported by the China Scholarship Council (CSC) under Grant 201406040058. The authors thank Jing Liu for the assistance in writing the paper. We thank the editor and anonymous reviewers for constructive feedback and the chance to improve the quality of our manuscript accordingly.

Appendix A. Supplementary data

Supplementary data to this article can be found online at https://doi.org/10.1016/j.rse.2018.02.029.

References

Ač, A., Malenovskỳ, Z., Olejníčková, J., Gallé, A., Rascher, U., Mohammed, G., 2015. Meta-analysis assessing potential of steady-state chlorophyll fluorescence for remote sensing detection of plant water, temperature and nitrogen stress. Remote Sens. Environ. 168, 420–436.

Asrar, G., Kanemasu, E.T., Miller, G.P., Weiser, R., 1986. Light interception and leaf area estimates from measurements of grass canopy reflectance. IEEE Trans. Geosci. Remote Sens. (1), 76–82.

Badgley, G., Field, C.B., Berry, J.A., 2017. Canopy near-infrared reflectance and terrestrial photosynthesis. Sci. Adv. 3 (3) e1602244.

Baker, N.R., 2008. Chlorophyll fluorescence: a probe of photosynthesis in vivo. Annu. Rev. Plant Biol. 59, 89–113.

Bartlett, D.S., Whiting, G.J., Hartman, J.M., 1989. Use of vegetation indices to estimate indices to estimate intercepted solar radiation and net carbon dioxide exchange of a grass canopy. Remote Sens. Environ. 30 (2), 115–128.

Berk, A., Anderson, G.P., Acharya, P.K., Bernstein, L.S., Muratov, L., Lee, J., Fox, M., Adler Golden, S.M., Chetwynd, J.H., Hoke, M.L., et al., 2005. MODTRAN 5: a reformulated atmospheric band model with auxiliary species and practical multiple scattering options: update. In: Defense and Security, pp. 662–667.

Cendrero-Mateo, M.P., Moran, M.S., Papuga, S.A., Thorp, K., Alonso, L., Moreno, J., Ponce-Campos, G., Rascher, U., Wang, G., 2015. Plant chlorophyll fluorescence: active and passive measurements at canopy and leaf scales with different nitrogen treatments. J. Exp. Bot. 67 (1), 275–286.

Damm, A., Guanter, L., Paul-Limoges, E., Van der Tol, C., Hueni, A., Buchmann, N., Eugster, W., Ammann, C., Schaepman, M., 2015. Far-red sun-induced chlorophyll fluorescence shows ecosystem-specific relationships to gross primary production: an assessment based on observational and modeling approaches. Remote Sens. Environ. 166, 91–105.

Fan, W., Liu, Y., Xu, X., Chen, G., Zhang, B., 2014. A new FAPAR analytical model based on the law of energy conservation: a case study in China. IEEE J. Sel. Top. Appl. Earth Observ. Remote Sens. 7 (9), 3945–3955.

Fournier, A., Daumard, F., Champagne, S., Ounis, A., Goulas, Y., Moya, I., 2012. Effect of canopy structure on sun-induced chlorophyll fluorescence. ISPRS J. Photogramm. Remote Sens. 68, 112–120.

Frankenberg, C., Fisher, J.B., Worden, J., Badgley, G., Saatchi, S.S., Lee, J.-E., Toon, G.C., Butz, A., Jung, M., Kuze, A., et al., 2011. New global observations of the terrestrial carbon cycle from GOSAT: patterns of plant fluorescence with gross primary productivity. Geophys. Res. Lett. 38 (17).

Gastellu-Etchegorry, J.-P., Lauret, N., Yin, T., Landier, L., Kallel, A., Malenovskỳ, Z., Al Bitar, A., Aval, J., Benhmida, S., Qi, J., et al., 2017. DART: recent advances in remote sensing data modeling with atmosphere, polarization, and chlorophyll fluorescence. IEEE J. Sel. Top. Appl. Earth Observ. Remote Sens.

Grace, J., Nichol, C., Disney, M., Lewis, P., Quaife, T., Bowyer, P., 2007. Can we measure terrestrial photosynthesis from space directly, using spectral reflectance and fluorescence? Glob. Chang. Biol. 13 (7), 1484–1497.

Guanter, L., Zhang, Y., Jung, M., Joiner, J., Voigt, M., Berry, J.A., Frankenberg, C., Huete, A.R., Zarco Tejada, P., Lee, J.-E., et al., 2014. Global and time-resolved monitoring of crop photosynthesis with chlorophyll fluorescence. Proceedings of the National Academy of Sciences 111 (14), E1327–E1333.

Hernández-Clemente, R., North, P., Hornero, A., Zarco-Tejada, P., 2017. Assessing the effects of forest health on sun-induced chlorophyll fluorescence using the FluorFLIGHT 3-D radiative transfer model to account for forest structure. Remote Sens. Environ. 193, 165–179.

Houborg, R., Soegaard, H., Boegh, E., 2007. Combining vegetation index and model inversion methods for the extraction of key vegetation biophysical parameters using Terra and Aqua MODIS reflectance data. Remote Sens. Environ. 106 (1), 39–58.

Huang, D., Knyazikhin, Y., Dickinson, R.E., Rautiainen, M., Stenberg, P., Disney, M., Lewis, P., Cescatti, A., Tian, Y., Verhoef, W., et al., 2007. Canopy spectral invariants for remote sensing and model applications. Remote Sens. Environ. 106 (1), 106–122.

Jacquemoud, S., 1993. Inversion of the PROSPECT + SAIL canopy reflectance model from AVIRIS equivalent spectra: theoretical study. Remote Sens. Environ. 44 (2–3), 281–292.

Jacquemoud, S., Baret, F., 1990. PROSPECT: a model of leaf optical properties spectra. Remote Sens. Environ. 34 (2), 75–91.

Jacquemoud, S., Verhoef, W., Baret, F., Bacour, C., Zarco-Tejada, P.J., Asner, G.P., François, C., Ustin, S.L., 2009. PROSPECT + SAIL models: a review of use for vegetation characterization. Remote Sens. Environ. 113, S56–S66.

Joiner, J., Yoshida, Y., Vasilkov, A., Middleton, E., et al., 2011. First observations of global and seasonal terrestrial chlorophyll fluorescence from space. Biogeosciences 8 (3), 637–651.

Knyazikhin, Y., Schull, M.A., Stenberg, P., Mõttus, M., Rautiainen, M., Yang, Y., Marshak, A., Carmona, P.L., Kaufmann, R.K., Lewis, P., et al., 2013. Hyperspectral remote sensing of foliar nitrogen content. Proc. Natl. Acad. Sci. 110 (3), E185–E192.

Koffi, E., Rayner, P., Norton, A., Frankenberg, C., Scholze, M., 2015. Investigating the usefulness of satellite-derived fluorescence data in inferring gross primary productivity within the carbon cycle data assimilation system. Biogeosciences 12 (13), 4067–4084.

Köhler, P., Guanter, L., Kobayashi, H., Walther, S., Yang, W., 2018. Assessing the potential of sun-induced fluorescence and the canopy scattering coefficient to track large-scale vegetation dynamics in Amazon forests. Remote Sens. Environ. 204, 769–785.

Krause, G., Weis, E., 1991. Chlorophyll fluorescence and photosynthesis: the basics. Annu. Rev. Plant Biol. 42 (1), 313–349.

Liu, L., Liu, X., Wang, Z., Zhang, B., 2016. Measurement and analysis of bidirectional SIF emissions in wheat canopies. IEEE Trans. Geosci. Remote Sens. 54 (5), 2640–2651.

Meroni, M., Rossini, M., Guanter, L., Alonso, L., Rascher, U., Colombo, R., Moreno, J., 2009. Remote sensing of solar-induced chlorophyll fluorescence: review of methods and applications. Remote Sens. Environ. 113 (10), 2037–2051.

Migliavacca, M., Perez-Priego, O., Rossini, M., El-Madany, T.S., Moreno, G., van der Tol, C., Rascher, U., Berninger, A., Bessenbacher, V., Burkart, A., et al., 2017. Plant functional traits and canopy structure control the relationship between photosynthetic CO_2 uptake and far-red sun-induced fluorescence in a Mediterranean grassland under different nutrient availability. New Phytol. 214 (3), 1078–1091.

Mõttus, M., Stenberg, P., 2008. A simple parameterization of canopy reflectance using photon recollision probability. Remote Sens. Environ. 112 (4), 1545–1551.

Porcar Castell, A., Tyystjärvi, E., Atherton, J., Van der Tol, C., Flexas, J., Pfündel, E.E., Moreno, J., Frankenberg, C., Berry, J.A., 2014. Linking chlorophyll a fluorescence to photosynthesis for remote sensing applications: mechanisms and challenges. J. Exp. Bot eru191.

Rautiainen, M., Stenberg, P., 2005. Application of photon recollision probability in coniferous canopy reflectance simulations. Remote Sens. Environ. 96 (1), 98–107.

Rossini, M., Nedbal, L., Guanter, L., Ač, A., Alonso, L., Burkart, A., Cogliati, S., Colombo, R., Damm, A., Drusch, M., et al., 2015. Red and far red sun-induced chlorophyll fluorescence as a measure of plant photosynthesis. Geophys. Res. Lett. 42 (6), 1632–1639.

Schull, M., Ganguly, S., Samanta, A., Huang, D., Shabanov, N., Jenkins, J., Chiu, J.C., Marshak, A., Blair, J., Myneni, R., et al., 2007. Physical interpretation of the correlation between multi-angle spectral data and canopy height. Geophys. Res. Lett. 34 (18).

Smolander, S., Stenberg, P., 2005. Simple parameterizations of the radiation budget of uniform broadleaved and coniferous canopies. Remote Sens. Environ. 94 (3), 355–363.

Stenberg, P., Manninen, T., 2015. The effect of clumping on canopy scattering and its directional properties: a model simulation using spectral invariants. Int. J. Remote Sens. 36 (19–20), 5178–5191.

Van der Tol, C., Rossini, M., Cogliati, S., Verhoef, W., Colombo, R., Rascher, U., Mohammed, G., 2016. A model and measurement comparison of diurnal cycles of sun-induced chlorophyll fluorescence of crops. Remote Sens. Environ. 186, 663–677.
Van der Tol, C., Verhoef, W., Timmermans, J., Verhoef, A., Su, Z., 2009. An integrated model of soil-canopy spectral radiances, photosynthesis, fluorescence, temperature and energy balance. Biogeosciences 6 (12), 3109–3129.
Van Wittenberghe, S., Alonso, L., Verrelst, J., Moreno, J., Samson, R., 2015. Bidirectional sun-induced chlorophyll fluorescence emission is influenced by leaf structure and light scattering properties — A bottom-up approach. Remote Sens. Environ. 158, 169–179.
Van Wittenberghe, S., Alonso, L., Verrelst, J., Veroustraete, F., Valcke, R., Moreno, J., Samson, R., 2012. Estimating fluorescence emission of city trees in valencia: from leaf to canopy level. European Geosciences Union General Assembly.
Verhoef, W., 1984. Light scattering by leaf layers with application to canopy reflectance modeling: the SAIL model. Remote Sens. Environ. 16 (2), 125–141.
Verhoef, W., 1985. Earth observation modeling based on layer scattering matrices. Remote Sens. Environ. 17 (2), 165–178.
Verrelst, J., Rivera, J.P., Van der Tol, C., Magnani, F., Mohammed, G., Moreno, J., 2015. Global sensitivity analysis of the SCOPE model: what drives simulated canopy-leaving sun-induced fluorescence? Remote Sens. Environ. 166, 8–21.
Verrelst, J., Van der Tol, C., Magnani, F., Sabater, N., Rivera, J.P., Mohammed, G., Moreno, J., 2016. Evaluating the predictive power of sun-induced chlorophyll fluorescence to estimate net photosynthesis of vegetation canopies: a SCOPE modeling study. Remote Sens. Environ. 176, 139–151.
Vilfan, N., van der Tol, C., Muller, O., Rascher, U., Verhoef, W., 2016. Fluspect-B: a model for leaf fluorescence, reflectance and transmittance spectra. Remote Sens. Environ. 186, 596–615.
Vogelmann, T., Han, T., 2000. Measurement of gradients of absorbed light in spinach leaves from chlorophyll fluorescence profiles. Plant Cell Environ. 23 (12), 1303–1311.
Yang, P., Verhoef, W., van der Tol, C., 2017. The mSCOPE model: a simple adaptation to the scope model to describe reflectance, fluorescence and photosynthesis of vertically heterogeneous canopies. Remote Sens. Environ. 201, 1–11.
Zarco-Tejada, P., Pushnik, J., Dobrowski, S., Ustin, S., 2003. Steady-state chlorophyll a fluorescence detection from canopy derivative reflectance and double-peak red-edge effects. Remote Sens. Environ. 84 (2), 283–294.
Zhang, Y., Guanter, L., Berry, J.A., Joiner, J., Tol, C., Huete, A., Gitelson, A., Voigt, M., Köhler, P., 2014. Estimation of vegetation photosynthetic capacity from space-based measurements of chlorophyll fluorescence for terrestrial biosphere models. Glob. Chang. Biol. 20 (12), 3727–3742.
Zhao, F., Dai, X., Verhoef, W., Guo, Y., van der Tol, C., Li, Y., Huang, Y., 2016. FluorWPS: a Monte Carlo ray-tracing model to compute sun-induced chlorophyll fluorescence of three-dimensional canopy. Remote Sens. Environ. 187, 385–399.